6 Iodo-Delta Lactone Inhibits Angiogenesis in Human HT29 Colon Adenocarcinoma xenograft.

Oglio Romina , Buschittari Federico , Salvarredi Leonardo , Michaux Jennifer , Rodriguez Carla , Perona Marina , Dagrosa Alejandra , Juvenal Guillermo , Thomasz Lisa

PII: S0952-3278(22)00119-3
DOI: https://doi.org/10.1016/j.plefa.2022.102507
Reference: YPLEF 102507

To appear in: *Prostaglandins, Leukotrienes and Essential Fatty Acids (PLEFA)*

Received date: 13 May 2022
Revised date: 24 August 2022
Accepted date: 6 October 2022

Please cite this article as: Oglio Romina , Buschittari Federico , Salvarredi Leonardo , Michaux Jennifer , Rodriguez Carla , Perona Marina , Dagrosa Alejandra , Juvenal Guillermo , Thomasz Lisa , 6 Iodo-Delta Lactone Inhibits Angiogenesis in Human HT29 Colon Adenocarcinoma xenograft., *Prostaglandins, Leukotrienes and Essential Fatty Acids (PLEFA)* (2022), doi: https://doi.org/10.1016/j.plefa.2022.102507

6 Iodo-Delta Lactone Inhibits Angiogenesis in Human HT29 Colon Adenocarcinoma xenograft.

Oglio Romina, Buschittari Federico, Salvarredi Leonardo, Michaux Jennifer, Rodriguez Carla, Perona Marina, Dagrosa Alejandra, Juvenal Guillermo, Thomasz Lisa.

[1]Department of Radiobiology (CAC), National Comission of Atomic Energy (CNEA), [2]National Council of Scientific and Technical Research (CONICET).

Grants: This work was supported by grants from the Argentine National Research Council (CONICET), the National Agency for the Promotion of Science and Technology (ANPCYT) and the National Atomic Energy Commission of Argentina (CNEA).

Corresonding author. Tel: 5411 67727187

E-mail address: thomasz@cnea.gov.ar, lisa75ar@yahoo.com.ar (L. Thomasz).

Highlights

IL-δ inhibits cell proliferation and induces apoptosis in human HT29 Colon adenocarcinoma xenograft.

IL-δ has an anti angiogenic effect in Colorectal cancer tumor vasculature.

The anti angiogenic effect of IL-δ involves a downregulation of VEGF and VEGF-R2 with an increased expression of Ang-1 and VEGF R1.

Author statement

Romina Oglio: Methodology, Investigation, Writing - Review & Editing. Federico Buschittari: Methodology. Leonardo Salvarredi: Formal analysis, Validation. Jennifer Michaux: Methodology. Carla Rodriguez: Writing. Marina Perona: Resources. Alejandra Dagrosa: Resources. Guillermo Juvenal: Supervision. Lisa Thomasz: Conceptualization, Investigation, Writing - Review & Editing.

Abstract

Introduction: Several studies have shown the antiproliferative effect of iodine and 5-hydroxy-6 iodo-eicosatrienoic delta lactone (IL-δ) on diverse tissues. It was demonstrated that molecular iodine (I_2) and IL-δ, but not iodide (I^-), exerts anti-neoplastic actions in different cancers. The underlying mechanism through which IL-δ inhibits tumor growth remains unclear. The aim of this study was to analyze the effect of IL-δ on tumor growth and angiogenesis in human HT29 colorectal cancer xenografts.

Methodology and Results: HT29 cells were injected subcutaneously into the flanks of nude mice and IL-δ was i.p. injected at a dose of 15 μg three days a week. IL-δ treatment in HT29 xenografts showed time-dependent inhibition of tumor growth, decrease of mitosis and PCNA expression ($p<0.05$), increase of P27 expression and Caspase 3 activity after 18 days of treatment ($p<0.05$). To assess tumor Microvessel Densities (MVD), CD31 staining by immunohistochemistry was analyzed. IL-δ treatment decreased MVD by 17% and 30% after 18 and 30 days respectively ($p<0.05$), as well as it decreased VEGF and VEGF-R2 expression ($p<0.05$). Additionally, our findings demonstrated that IL-δ increased VEGF-R1 and Ang-1 mRNA levels ($p<0.01$).

Conclusion: The antitumor efficacy of IL-δ in vivo involves inhibition of cell proliferation as well as induction of apoptosis. IL-δ has also anti-angiogenic effect associated with VEGF and VEGF-R2 downregulation followed by Ang-1 and VEGF-R1 increased expression. High levels of Ang-1 would contribute to mature vessel stabilization and maintenance while VEGF-R1 increase would produce anti-proliferative effect on endothelial cells.

Keywords: Iodolipids, Iodolactone, Colon cancer, angiogenesis.

1. Introduction

Several studies have shown the anti-proliferative effect of iodine and an iodinated derivative of arachidonic acid (AA), 5-hydroxy-6-iodo-8,11,14-eicosatrienoic acid, delta iodolactone (IL-δ) on different tissues [1, 2]. It was demonstrated that molecular iodine (I_2) and IL-δ, but not iodide (I^-), exert anti-neoplastic actions in different cancers [3, 4]. The antineoplastic effect of iodine could be due to the synthesis of intracellular iodinated lipids [5]. Iodide can generate IL-δ only in cells expressing specific transporters and peroxidases as it must be oxidized to derive into iodinated compounds to induce cytotoxic effects [6-8].

It has been shown that IL-δ exhibits anti-tumor properties in breast cancer, prostate cancer, neuroblastoma, glioblastoma, melanoma, lung and thyroid carcinoma cells [9, 10]. The anti-proliferative action of I_2 and IL-δ in vitro, could be associated with apoptosis in several human

cancer cell lines [11, 12]. In some instances, iodine and IL-δ induce apoptosis through a mitochondrial mechanism [13].

In breast cancer, Arroyo-Helguera et al., (2006) showed that IL-δ increased four times its antiproliferative action compared to I_2 [9]. Furthermore, the mechanism involved could be through the peroxisome proliferator-activated receptors (PPAR) [14, 15]. Actually, IL-δ is a specific ligand of the PPAR gamma isoform (PPARγ), presenting a six times affinity increase compared to arachidonic acid (AA). This data suggests that IL-δ/PPARγ could participate in the anti-proliferative and pro-apoptotic effect of IL-δ [16].

In thyroid cancer cells, IL-δ induced loss of cell viability while promoting apoptosis and reactive oxygen species (ROS) generation [17]. However, different sources of ROS were observed. The anti-proliferative effect of IL-δ on a thyroid papillary cancer cell line (TPC-1) involves mitochondria-mediated ROS production, while in a thyroid follicular cancer cell line (WRO) it is related to NOX-4 expression [17].

In previous reports, we also observed that IL-δ induced apoptosis through (ROS) generation in the HT29 colorectal cancer cell line without any detectable effects of its precursors: AA and KI [18]. Moreover, IL-δ also induced a significant tumor growth delay in HT29 xenografts.

The aim of this study was to analyze the effect of IL-δ on angiogenesis and the relationship between tumor growth and blood-vessel formation in human colorectal cancer cell line HT29 via a tumor xenograft model in athymic nude mice.

2. Materials and Methods

2.1. Chemical synthesis of IL- δ

Chemical synthesis of IL-δ was based on a modification of Monteagudo et al., method (1990). Briefly, iodine (156 mg) was added to a solution of AA (65 mg) in acetonitrile (0.8 mL) at 4 ºC.

The solution was kept under N_2, stirred for 4 h at room temperature and protected from light. The solution containing crude product was concentrated under low nitrogen flow to 0.5 ml and separated on silica gel column and preparative TLC using the solvent system CH2Cl2/MeOH (97.5:2.5). The IL-δ synthesized was concentrated under low nitrogen flow. Before use the IL-δ was diluted in RPMI, sonicated and carried to a final concentration of 10 mM. IL-δ is stable under the present experimental conditions [19].

2.2. *In vivo* tumorigenicity assay

Each experimental group included 7 homozygous female NIH-nude mice, 20–25 g b.w., 6-8 weeks of age, bred and maintained in laminar air-flow racks. HT29 cells were harvested and injected subcutaneously into the flanks of the mice. Tumors were allowed to developed during the following 7 days. When tumors were palpable, mice were treated with IL-δ (15 μg i.p., three days a week).The size of the tumors was measured with a caliper twice a week, and the volume was calculated according to the following formula: A2 x B/2 (where A is the width and B is the length). The mice were sacrificed 18 and 30 days post IL-δ injection. The studies were performed in accordance with International Helsinki Code and the NIH guidelines and the ethics guidelines suggested by the Argentinean Association of Science and Laboratory Animals. The study was approved by the Institutional Animal Care and Use Committee of the CNEA.

2.3. Histological analysis

After fixation, tissues were dehydrated and embedded in Histoplast Biopack (Buenos Aires, Argentina), and tissue sections (5–8 μm) were placed in 3-aminopropyltrietoxysilane (Sigma-Aldrich, Merck KGaA, and Darmstadt, Germany) coated slides and stained with Hematoxylin-Eosin (H&E). Digital pictures were captured with an Olympus BX51 microscope coupled with an Olympus DP70 camera. Images from necrotic and viable areas were taken from 1 to 3 histological sections per tumor with a 4X objective and analyzed using the free software ImageJ Version 1.42 (National Institutes of Health, USA). The ratios between the necrotic and viable area (na/va) were evaluated after 30 days of IL-δ treatment. Mitosis was evaluated by counting the total number of mitotic figures in histological sections stained with H&E of 10 microscopic fields (40X objective).

2.4. Western blot analysis

Proteins were extracted in lysis buffer RIPA (50mM Tris-HCl pH 7.4, 150mM NaCl, 1% Nonidet P40, 0.1% SDS, 0.5% deoxycholate), supplemented with PMSF 0.5 mM and protease inhibitor cocktail (Sigma-Aldrich). Thirty micrograms of total proteins were electrophoresed on 10% polyacrylamide gels and transferred to PVDF membranes. Membranes were blocked with 5% BSA in phosphate buffer saline solution (PBS) with 0.2% Tween 20 (Sigma) for 1 h at room temperature and then incubated overnight at 4 ºC with monoclonal anti PCNA antibodies (dilution 1:500, Santa Cruz Biotechnology) and anti P27 (dilution 1:500, Calbiochem, USA). Next day, Membranes were washed, incubated for 1 h at room temperature with peroxidase-labeled (HRP)secondary antirabbit or antimouse antibody (1:2,000; Santa Cruz, CA, USA), and visualized with the enhanced

chemiluminescence method. Densitometric analysis was performed using the NIH ImageJ analysis Software (1.40g Wayne Rasband, National Institute of Health, USA) and results were normalized to β-actin expression.

2.5. Caspase-3 activity

Caspase-3 activity was determined with the Caspase-3 Assay kit, according to the manufacturer's instructions (Sigma CASP-3-C, Sigma-Aldrich, St. Louis, Mo, USA). This assay is based on the spectrophotometric detection of the Ac-DEVD-pNA (p-nitroaniline) substrate after cleavage. Tumors were harvested in lysis buffer [50 mm HEPES, 5 mM dithiothreitol (DTT), 5mN CHAPS, 10 μg/mL pepstatin, benzamidine 2.5 mM, aprotinina 10 μg/mL, pepstatin 1 μg/mL, 0,5 mM phenylmethylsulfonylfluoride (PMSF), pH 7.4] and homogenized with a Teflon-glass homogenizer. Lysates were clarified by centrifugation at 10,000 x *g* for 5 min, and clear lysates containing 100 μg proteins were incubated with caspase-3 substrate, at 37°C for 3 h. The concentration of the p-nitroaniline (pNA) released from the substrate is calculated from the absorbance values at 405 nm after incubating the plate at 37°C for 90 min. The activity, expressed as micromoles of p-nitroaniline per minute per milliliter, was calculated with a p-nitroaniline calibration curve. A positive control of caspase-3 and an inhibitor of caspase-3 (200 mmol/L Inhibitor Acetyl-Asp-Glu-Val-Asp-al [Ac-DEVD-CHO]) were also used.

2.6. Immunostaining

Paraffin sections were deparaffinized and rehydrated. Antigen retrieval was done by heating samples in a microwave for 15 min in 0.01 M citrate buffer (pH 6.0). Endogenous peroxidase activity was blocked by applying 3% hydrogen peroxide. After 30 min of blocking with horse serum, the primary antibody [VEGF (abcam sc-507, 1:100), CD31 (abcam sc-507, 1:100), and VEGF-R2 (abcam sc-504, 1:100)] was applied followed by overnight incubation at 4C. Negative controls were processed excluding the primary antibody. Slides were washed three times with phosphate buffered saline (PBS) for 5 min. The biotinylated secondary antibody and the streptavidin–biotin complex (Vector Laboratories, Burlingame, CA) were then applied. After rinsing with PBS, the slides were immersed for 5 min in the coloring substrate 3,3#-diaminobenzidine (Sigma) at 0.4 mg/ml with 0.003% hydrogen peroxide, rinsed with distilled water, counterstained with hematoxylin, dehydrated and covered.

Microvessels density (MVD) was measured using immunohistochemistry with an anti-mouse CD31 antibody. Any brown-stained tubular structure or endothelial cell cluster was counted as one microvessel using a freehand selection. Vascularity was measured by the average number of vessels

per field counted in 10 random areas. The images for quantifications were taken in the same conditions using a 20X objective. Only areas of viable tumor tissues were imaged. The scoring of the slides was determined by two independent observers who were blinded to the identity of the slides using the free software ImageJ Version 1.42 (National Institutes of Health, USA). MVD was calculated as the average number of vessels per field. The average vascular area (AVA) of each vessel was counted in 10 random areas with a 20X objective.

The VEGF expressed in the cytoplasm of tumor cell and VEGF-R2 expression was quantified using the free software ImageJ Version 1.42.The images for quantifications were taken in the same conditions using a 40X objective. Images were transformed to grayscale and the Integrated Intensity per field was analyzed in five random fields per slide. Background correction was performed manually by substracting a negative square area in each final image.

2.7. RNA extraction and real-time PCR

Extraction and purification of RNA were performed following the TRIzol method. 2.5 μg RNA were used as a template for cDNA synthesis with Oligo $(dT)_{20}$ using the Superscript III reverse transcriptase (Invitrogen). cDNA (1 μl, 1/10) was used in each PCR reaction in a total volume of 25μL, with specific primers for the target molecules and the Real Time Master Mix (Promega). Real-time PCR was carried out using a Rotor-gene Q analyzer (Qiagen). Specific primers pairs for each gene analyzed and temperature of annealing are listed below, GADPH: forward 5′-ACAGCAACAGGGTGGTGGAC-3′ and reverse 5′-TTTGTGGGTGCAGCGAACTT-3′ (57°C), VEGFA: forward 5′-GCAGCGACAAGGCAGACTAT-3′ and reverse 5′-AACCTCCTCAAACCGTTGGC-3′ (59ºC), VEGF-R1: forward 5′-ACGGTTAGCACATTGGTGGT-3′ and reverse 5′-CGGCTGGCATCTTTTCCAAG-3′ (59ºC), VEGF-R2: forward 5′-GACCAAGAGTGACCAAGGGG-3′ and reverse 5′-GATTCGGACTTGACTGCCCA-3′ (60ºC), Ang-1 forward 5′-TTCCGTAGGGGGCATTTGTG-3′ and reverse 5′-GGCCGTGTGGTTTTGAACAG-3′ (58ºC). Relative changes in gene expression were calculated according to the $2^{-\Delta\Delta Ct}$ method using GADPH as internal control.

2.8. Statistical analysis

Results are expressed as mean ± SD. Statistical analysis of the results was made by one way ANOVA followed by Student-Newman-Keuls test. Differences were considered significant at $p<0.05$.

3. Results

3.1. The anti-tumor effects of IL-δ correlate with the decrease of PCNA expression and increase of apoptosis

Increase evidence demonstrated that delta-Iodolactone (Fig.1A) exerts its antiproliferative and apoptotic effects not only in thyrocytes but also in other cell types. To further characterize the process by which IL-δ inhibits tumor growth, we analyzed the anti-proliferative and apoptotic effects of IL-δ in HT29 xenografts. In previous studies, we demonstrated that a daily administration of IL-δ (15 µg) inhibits tumor growth in a time-dependent way [18]. In this study, we administered 15 µg of IL-δ three times a week. The results shown in Figure1B and 1C, demonstrated that IL-δ significantly inhibits tumor growth in HT29 xenografts. As shown in Fig. 1D, the histological analysis revealed that IL-δ administration reduce the ratio between the necrotic and viable area (na/va) after 30 days ($p<0.05$). To determinate mitosis index we evaluated total number of mitosis per field after 18 days. A decrease of mitotic index was observed in Fig. 2A and 2B. Then, we analyzed the expression of protein markers for cell proliferation, the proliferating cellular nuclear antigen (PCNA) and the CDK inhibitor p27 by Western blot. As shown in Fig. 2C and 2D, IL-δ caused a significant decrease of PCNA ($p<0.05$) and a significant increase of P27 expression ($p<0.05$) after 18 days of treatment. To analyze apoptosis, we quantified caspase-3 activity. In Fig. 2E, caspase-3 activity values were 20 % higher after 18 days of IL-δ treatment compared to control group ($p<0.05$). These findings suggest that antitumor efficacy of IL-δ involved both inhibition of cell proliferation as well as apoptosis induction.

3.2. IL-δ inhibits angiogenesis in HT29 xenograft model

To evaluate the effect of IL-δ on angiogenesis, we assess the tumor microvessel densities (MVD). For this purpose, we analyzed tumors CD31 stained cells, an endothelial cell-specific marker (Fig. 3A). The IL-δ treatment decreased MVD by 15 % compared to control group after 18 days and by 30% ($p<0.05$) after 30 days (Fig. 3B). We also analyzed the average vascular area (AVA). The AVA decreased as the tumor volume increased and only a slight decreased of AVA after 30 days of IL-δ treatment was observed (Fig. 3C).

3.3. IL-δ decrease VEGF and VEGF-R2 expression in HT29 xenograft model

To further characterize the vascularization during tumor growth inhibition, we decided to explore the role of the vascular endothelial growth factor (VEGF) and VEGF–receptor system. Real-time PCR analyses revealed decreased VEGF and VEGF-R2 levels after 30 days of IL-δ treatment ($p<0.05$) (Fig. 4A,4B). Immunohistochemistry analysis showed that IL-δ decreased the integrated intensity of VEGF-stained cells by 47 % (n.s) after 18 days of treatment and 80 % ($p<0.05$) after 30 days of treatment (Fig. 4C, 4D). On the other hand, VEGF-R2 integrated intensity was reduced by 82 % ($p<0.01$) after 30 days of treatment (Fig. 4E, 4F).

3.4. IL-δ increased VEGF-R1 and Ang-1

Given that VEGF-R1 and Ang-1 are associated with endothelial dysfunction and vascular remodeling, we analyzed the expression of both. Real time PCR revealed that IL-δ treatment increased VEGF-R1 and Ang-1 mRNA. Figure 5A shows that IL-δ treated mice expressed 70 % higher levels of VEGF-R1 mRNA than control group after 18 days of treatment ($p<0.05$) and 50 % higher levels of VEGF-R1 mRNA than control group after 30 days of IL-δ treatment ($p<0.01$). As shown in Fig. 5B, IL-δ also increased Ang-1 mRNA levels by 30% after 18 days ($p<0.01$) and 60 % after 30 days ($p<0.01$) compared to their respective time control group.

4. Discusion

These results confirm our previous observations that IL-δ treatment inhibits cell proliferation and induces apoptosis in HT29 cell line [18]. In the present study, we have extended our observations to investigate the in vivo consequences of IL-δ treatment on angiogenesis.

First, we analyzed different parameters, such as: tumor growth, mitotic index, and the expression of proliferating cell nuclear antigen (PCNA), involved in DNA replication, and p27, a CDK regulator that controls cell division. We have also evaluated apoptosis and the ratio between the necrotic and viable area. We corroborated that IL-δ inhibits tumor growth in a time-depend manner in this model. The IL-δ treatment reduced the mitotic index, decreased PCNA expression and increased P27 levels. These observations could suggest a possible induction of cell cycle arrest since the increase in p27 levels are associated with cell cycle arrest in G1 [20]. In addition, decreased PCNA may indicate an abnormality during the G1/S cell-cycle transition [21]. Although, the effect of IL-δ on the cell cycle in HT29 cells was not evaluated here, it has been shown that IL-δ can induce cell cycle arrest in G1 or G2/M phases in normal and cancerous breast cells [4]. In HT29 cells, more studies are required to provide further evidence to elucidate this mechanism. However, it has been

proposed that the peroxisome proliferator-activated receptors gamma (PPARγ) could be the mediator of IL-δ effects, such as proliferation, apoptosis and angiogenesis [15, 16]. In this sense, IL-δ has six times more affinity for the PPARγ isoform than AA in vitro [22]. PPARγ stimulation is triggered by endogenous and exogenous ligands and it is able to inhibit cell proliferation, induce cell cycle arrest and apoptosis of multiple cancer cell lines [23]. Here, the induction of apoptosis was evidenced by an increase in caspase-3 activity. This result is in agreement with our earlier study, in vitro, on HT29 cells treated with IL-δ. The anti-proliferative and pro-apoptotic effects of IL-δ on colorectal cancer are consistent with those reported in other tumoral cell lines. Rosner et al., 2010 [10] have described that IL-δ has antitumor properties in breast cancer, neuroblastoma, glioblastoma, melanoma and lung carcinoma cells. Aranda et al., 2013 [8] also showed apoptotic effects of IL-δ in human prostate cancer cell lines. Taken together, these findings suggest that antitumor efficacy of IL-δ involves both inhibition of cell proliferation as well as induction of apoptosis.

It is known that, in in vivo tumor growth, there are ischemic and necrotic areas associated with increased tumor size and poor prognosis. We found a decrease of necrotic area due to the reduction of tumor mass induced by IL-δ. It will be crucial for the development of the therapeutic strategy since necrotic cells release molecules which exert tumor-promoting activity by inducing angiogenesis, proliferation, and invasion [24].

Angiogenesis is one of the most important characteristics of tumor growth. The growing tumor mass must be supplied by a vascular net that delivers nutrients and oxygen into it. Here, angiogenesis was preferentially assessed by immunodetection of the endothelial marker CD31. We found a significant decrease in microvessel densities (MVD) in tumors of IL-δ treated mice. These results suggest a role of IL-δ treatment in colorectal cancer tumor vasculature.

The decrease in VEGF and VEGF-R2 expression induced by IL-δ, might explain the changes in MVD and thus tumor vasculature. It is well known that VEGF promotes microvascular development and that its over-expression was related to higher vessel count in cancer [25-28]. Indeed, VEGF plays a critical role in colon cancer growth via angiogenesis by promoting endothelial cell growth, migration and survival, which is responsible for vascularizing colon tumors [29-31].

In addition, mRNA expression levels of VEGF-R1 and Ang-1 were analyzed. We showed that VEGF-R1 expression is positively correlated with the anti-proliferative effects of IL-δ and Caspase-3 activity. Previous reports suggested that soluble VEGF-R1 has apoptotic effects on endothelial cells and induces tumor injury [32]. Additionally, our findings showed that IL-δ treatment increases VEGF-R1 and Ang-1 expression and that it is negatively correlated with the MVD decrease in

HT29 tumor cells. The increased expression of VEGF-R1 and Ang-1 could be associated with apoptosis induction and the inhibitory effect of IL-δ on angiogenesis. However, further studies are needed to define this process.

Although, the precise role of VEGF-R1 in endothelial cells is still being elucidated, some studies suggested that the negative role of VEGF-R1 in angiogenesis is associated with its ability to alter endothelial cell division [33, 34]. It has been described that VEGF-R1 induces endothelial dysfunction, vascular remodeling, endothelial repair and regeneration mechanisms [35, 36]. Interestingly, the ability of VEGF-R1 to stimulate biological responses either negative or positive is limited to its ability to heterodimerize with VEGF-R2. Moreover, it has been described that VEGF-R1 anti-angiogenic effect could be due to its decoy activity, acting as an extracellular receptor of VEGF, modulating VEGF-R2 function [25]. Tatsuya Miyake et al., 2016 [37] also describe a direct damage effect caused by soluble VEGFR-1 on ovarian and colorectal cancers cells and suggest that soluble VEGFR-1 is an anti-angiogenic agent. They also propose VEGFR-1 as a potential cancer therapeutic candidate.

Nevertheless, the increased levels of Ang-1 in IL-δ in treated mice could also be responsible, in part, for the decrease on angiogenesis. This hypothesis is in line with Ahmad et al., 2001 [38], who observed that HT29 colon tumors produced by the Ang-1 transfectants had fewer vessels and lower tumor cell proliferative indexes than control tumors group. They hypothesize that an overproduction of Ang-1 inhibits or slows angiogenesis because of this stabilizing effect. Ang-1 is involved in endothelial cell migration, adhesion, and the recruitment of pericytes and smooth muscle cells, while Ang-2 is a vessel destabilizer [39]. However, the role of Ang-1 in tumor angiogenesis is controversial. In fact, its overexpression stimulates divergent responses depending on tumor type, ranging from promotion to limitation of growth [40]. Stoeltzing et al., 2003 suggest that Ang-1 is an important regulator of angiogenesis and vascular permeability and that this effect may be secondary to increasing peri endothelial support and vessel stabilization [39]. Conversely, overproduction of Ang-2, from any cell type, may induce angiogenesis and subsequent tumor growth in an in vivo system.

Several pathways could be proposed to explain the IL-δ effects on angiogenesis. Inhibition of type 2 cyclooxygenase (Cox2) could be another proposed mechanisms associated with iodine and IL-δ anti-angiogenic effects [22]. Indeed, prostaglandin E2, a major product of cyclooxygenase, has been implicated in modulating angiogenesis, vascular function, and inflammatory processes [41]. Accumulated evidence shows inhibition of angiogenesis by PPARγ agonists [42]. Although PPARγ could be stimulated by IL-δ in HT29 cells, more studies are required to provide further evidence to elucidate if PPARγ is involved.

The present results showed that IL-δ caused reduction of tumor mass and microvessel densities resulting in angiogenesis decrease. In the present study we demonstrated downregulation of VEGF and VEGF-R2 associated with Ang-1 and VEGF-R1 increased expression. High levels of Ang-1 would contribute to mature vessel stabilization and maintenance while VEGF-R1 increase would produce anti-proliferative effect on endothelial cells. Based on the role of angiogenesis in tumor formation and the mechanisms of action of anticancer agents, it is possible that these findings might explain, at least in part, the antiangiogenic effect of IL-δ. Taken together the data described above, it is also reasonable to speculate that IL-δ could be used as a chemotherapeutic agent for the treatment of cancer tissues, alone or in combined therapies.

Conflict of interest

The authors have no conflict of interest to declare.

Acknowledgments

This work was supported by grants from the Argentine National Research Council (CONICET), the National Agency for the Promotion of Science and Technology (ANPCYT) and the National Atomic Energy Commission of Argentina (CNEA).

References

[1] A. Dugrillon, W.M. Uedelhoven, M.A. Pisarev, G. Bechtner, R. Gärtner. Identification of delta-iodolactone in iodide treated human goiter and its inhibitory effect on proliferation of human thyroid follicles. Horm Metab Res. 1994. 26(10):465-9.

[2] L. Thomasz, R. Oglio, A.S. Randi, M. Fernandez, M.A. Dagrosa, R.L. Cabrini RL, G.J. Juvenal, Pisarev MA. Biochemical changes during goiter induction by methylmercaptoimidazol and inhibition by delta-iodolactone in rat. Thyroid, 2010 Sep;20(9):1003-13.

[3] H. Rösner, M. Wolfgang, S. Groebner, P. Torremante. Antiproliferative/cytotoxic effects of molecular iodine, povidone-iodine and Lugol's solution in different human carcinoma cell lines. Oncology Letters. 2016. 12, 2159-2162.

[4] O. Arroyo-Helguera, E. Rojas, G. Delgado, C. Aceves. Signaling pathways involved in the antiproliferative effect of molecular iodine in normal and tumoral breast cells: Evidence that 6-iodolactone mediates apoptotic effects. Endocr Relat Cancer. 2008. 15, 1003-1011.

[5] M. Nava-Villalba, C. Aceves. 6-iodolactone, key mediator of antitumoral properties of iodine. Prostaglandins Other Lipid Mediat (2014)112:27-33.

[6] M.A. Pisarev.,R. Gartner. Autoregulatory action of iodine. In: Braverman, L.E., Uitger, R.D. (Eds.), The Thyroid, 9th ed. Lippincott, Philadelphia,2000, pp. 85–90.

[7] V. Panneels, G. Juvenal, G., J.M. Boeynaems, J.E., Dumont, J. Van Sande. Iodide effects on the thyroid. In: Preedy, V.R., Burrow, G.N., Watson, R. (Eds.), Comprehensive Handbook on Iodine: Nutritional, Endocrine and Pathological Aspects. Oxford Academic Press, 2009, pp. 99305–99316.

[8] N. Aranda, S. Sosa, G. Delgado, C. Aceves, B. Anguiano. Uptake and antitumoral effects of iodine and 6-iodolactone in differentiated and undifferentiated human prostate cancer cell lines. Prostate. 2013. 73, 31–41.

[9] O. Arroyo-Helguera, B. Anguiano, G. Delgado, C. Aceves. Uptake and antiproliferative effect of molecular iodine in the MCF-7 breast cancer cell line. Endocr. Relat. Cancer (2006) 13, 1147–1158.

[10] H. Rösner, P. Torremante, W. Möller and R. Gärtner. Antiproliferative/cytotoxic activity of molecular iodine and iodolactones in various human carcinoma cell lines. No interfering with EGF-signaling, but evidence for apoptosis. Exp Clin Endocrinol Diabetes (2010) 118, 410-419.

[11] R. Gartner,P. Rank, B. Ander. The role of iodine and delta-iodolactone in growth and apoptosis of malignant thyroid epithelial cells and breast cancer cells. Hormones (2010) 9, 60–66.

[12] R. Langer, C. Burzler, G. Bechtner, R. Gartner. Influence of iodide and iodolactones on thyroid apoptosis. Evidence that apoptosis induced by iodide is mediated by iodolactones in intact porcine thyroid follicles. Exp. Clin. Endocrinol. Diabetes. (2003) 111, 325–329.

[13] A. Shrivastava, M, Tiwari, Sinha, R.A., Kumar, A.K Balapure, V.K Bajpai, R. Sharma, K. Mitra, K., A. Tandon, and M.M. Godbole. Molecular iodine induces caspase-independent apoptosis in human breast carcinoma cells involving mitochondria-mediated pathway. J BiolChem. 2006. 28, 19762-19771.

[14] C. Aceves, P. García-Solís, O. Arroyo-Helguera, L. Vega-Riveroll, G. Delgado, B. Anguiano. Antineoplastic effect of iodine in mammary cancer: participation of 6-iodolactone (6-IL) and peroxisome proliferator activated receptors (PPAR). Mol. Cancer (2009) 8,33-42.

[15] M. Nava-Villalba, R.E. Nuñez-Anita, A. Bontempo, C. Aceves, C. Activation of peroxisome proliferator-activated receptor gamma is crucial for the antitumor effect of 6-iodolactone. Mol Cancer. 2015. 14, 168-172.

[16] R. Nuñez-Anita, O. Arroyo-Helguera, M. Cajero-Juárez, L. López-Bojorquez, C. Aceves, C. A complex between 6-iodolactone and the peroxisome proliferator-activated receptor type gamma may mediate the antineoplasic effect of iodine in mammary cancer. Prostaglandins Other Lipid Mediat (2009) 89, 34–42.

[17] L. Thomasz, R. Oglio, L. Salvarredi, M. Perona, L. Rossich, S. Copelli, M. Pisarev, G. Juvenal. Regulation of NADPH oxidase NOX4 by delta iodolactone (IL-δ) in thyroid cancer cells. Mol Cell Endocrinol (2018)15,115-126.

[18] L. Thomasz, R. Oglio, L. Rossich, V. Villamar, M. Perona, L. Salvarredi, M.A. Pisarev, G.J. Juvenal. . 6 Iodo-d-lactone: a derivative of arachidonic acid with antitumor effects in HT29 colon cancer cells. Prostaglandins Leukot. Essent. Fatty Acids. (2013) 88, 273– 280.

[19] L. Thomasz , R. Oglio, A. Dagrosa, L. Krawiec, M.A. Pisarev, G. Juvenal. 6 iodo-d- lactone reproduces many but not all the effects of iodide. Mol Cell Endocrinol. (2010) 29;323(2):161-6.

[20] A.M. Abukhdeir, B.H. Park. P21 and P27: roles in carcinogenesis and drug resistance. Expert Rev Mol Med. (2008) jul 1; 10:19.

[21] H.J. Choi, I.K. Jung, S.S. Kim, and S.H. Hong, "Proliferating cell nuclear antigen expression and its relationship to malignancy potential in invasive colorectal carcinomas," Diseases of the Colon & Rectum, (1997) vol. 40, no. 1, pp. 51–59.

[22] C. Aceves, I. Mendieta, B. Anguiano and E. Delgado-González. Molecular Iodine Has Extrathyroidal Effects as an Antioxidant, Differentiator, and Immunomodulator. Int. J. Mol. Sci (2021) 22,1228-1243.

[23] T. Chi, M. Wang, X. Wang, K. Yang, F. Xie, Z. Liao, P. Wei. PPAR-γ Modulators as Current and Potential Cancer Treatments. Front Oncol. (2021) Sep 23;11:737776.

[24] S.Y. Lee, M.K. Ju , H.M. Jeon, E.K. Jeong, Y.J. Lee, C.H. Kim, H.G. Park, S.I. Han , H.S.Kang. Regulation of Tumor Progression by Programmed Necrosis. Oxid Med Cell Longev. (2018) Jan 31;2018:3537471.

[25] N. Rahimi. VEGFR-1 and VEGFR-2: two non-identical twins with a unique physiognomy. Front Biosci. (2006) 11, 818–829.

[26] C. Benazzi,1 A. Al-Dissi, C.H. Chau, W.D. Figg, G. Sarli, J.T. de Oliveira, and F. Gärtner. Angiogenesis in Spontaneous Tumors and Implications for Comparative Tumor Biology. Scientific World Journal (2014)2014,1-16.

[27] J.S. Lewis, R.J. Landers, J.C.E. Underwood, A.L. Harris. Expression of vascular endothelial growth factor by macrophages is up-regulated in poorly vascularized areas of breast carcinomas. Journal of Pathology (2000), 192, 150e158.

[28] Manoj Kumar Gupta, Ren-Yi Qin. Mechanism and its regulation of tumor-induced angiogenesis .World J Gastroenterol (2003), 9:1144-1155.

[29] H. Saman, S.S. Raza, S. Uddin and K. Rasul. Inducing Angiogenesis, a Key Step in Cancer Vascularization, and Treatment Approaches. Cancers (2020) 12, 1172-1184.

[30] Weijing Sun. Angiogenesis in metastatic colorectal cancer and the benefits of targeted therapy. Journal of Hematology & Oncology (2012) 5:63-72.

[31] L. Zhiyong, Q. Lisha, L. Yixiani, Z. Xiulan and S. Baocun. VEGFR2 regulates endothelial differentiation of colon cancer cells. BMC Cancer (2017) 17:593-604.

[32] M. Shibuya, M. Vascular endothelial growth factor receptor-1 (VEGFR-1/Flt-1): a dual regulator for angiogenesis. Angiogenesis. 2006. 9,225–230.

[33] J.B. Kearney, C.A. Ambler, K.A. Monaco, N. Johnson, R.G. Rapoport, V.L. Bautch . Vascular endothelial growth factor receptor Flt-1 negatively regulates developmental blood vessel formation by modulating endothelial cell division. Blood (2002), 99:2397–407.

[33] G. Di Marco 1, S. Reuter, U. Hillebrand, S. Amler, Maximilian König, E. Larger, H. Oberleithner, E. Brand, H. Pavenstädt, M. BrandG. The soluble VEGF receptor sFlt1 contributes to endothelial dysfunction in CKD. J. Am. Soc. Nephrol. (2009), 20; 2235–2245.

[34] H. Chen, et al. Inhibition of vascular endothelial growth factor activity by transfection with the soluble FLT-1 gene. J. Cardiovasc. Pharmacol.(2000) 36, 498–502.

[35] G.H. Fong, J. Rossant, M. Gertsenstein, M.L. Breitman. Role of the Flt-1 receptor tyrosine kinase in regulating the assembly of vascular endothelium. Nature (1995)376:66–70.

[37] T. Miyake, K. Kumasawa, N. Sato, T.Takiuchi, H. Nakamura, T. Kimura. Soluble VEGF receptor 1 (sFLT1) induces non-apoptotic death in ovarian and colorectal cancer cells. Sci Rep.(2016) 6:24853-24863.

[38] S.A. Ahmad 1, W. Liu, Y.D. Jung, F. Fan, M. Wilson, N. Reinmuth, R.M. Shaheen, C.D. Bucana, L.M. Ellis . The effects of angiopoietin-1 and -2 on tumor growth and angiogenesis in human colon cancer. Cancer Res. (2001)15:1255-9.

[39] O. Stoeltzing et. al. Angiopoietin-1 inhibits vascular permeability, angiogenesis, and growth of hepatic colon cancer tumors. Cancer Res. (2003) 15:3370-7.

[40] R.G. Akwii, M.S. Sajib, F.T. Zahra, C.M. Mikelis. Role of Angiopoietin-2 in Vascular Physiology and Pathophysiology Cancer Res. Cells (2019) 8, 471-490.

[41] S.Namkoong, S.J. Lee, C.K. Kim, Y.M. Kim, H.T. Chung, H. Lee, J.A. Han, K.S. Ha, Y.G. Kwon, Y.M. Kim. Prostaglandin E2 stimulates angiogenesis by activating the nitric oxide/cGMP pathway in human umbilical vein endothelial cells. Exp Mol Med. (2005) Dec 31;37(6):588-600.

[42] D. Panigraphy, S. Huang, M. W. Kieran & A. Kaipainen. PPARγ as a therapeutic target for tumor angiogenesis and metastasis. Cancer Biology & Therapy (2005)7, 687-693.

Figures

Figure 1. **IL-δ inhibits HT29 tumor growth.** A) Representative molecule of 5-hydroxy-6 iodo-eicosatrienoic delta lactone. B) Effect of IL-δ in tumor growth. HT29 cells were injected into the right flank of nude mice. After tumor development, mice were treated with IL-δ (15 µg) or vehicle three days a week. Points: mean tumor size; bars: SD, * $p<0.05$, ** $p<0.01$ versus control. C) Tumor tissues with skin were removed and photographed after 7, 18 and 30 days of treatment. D) Hematoxylin and Eosin (H&E) stained sections from tumors after 30 days of control and IL-δ

treatment. E) Relationship between necrotic area and viable area (na/va) after 30 days of IL-δ treatment (*$p<0.05$ versus control).

FIGURE 1

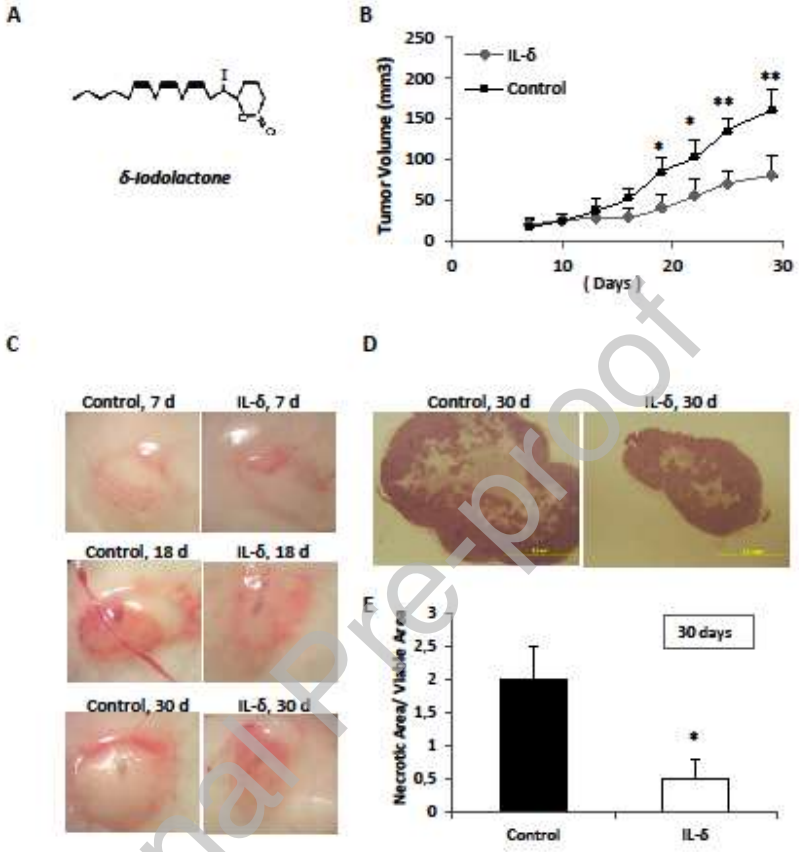

Figure 2. **IL-δ inhibits cell proliferation.** A) Representative micrographs of IL-δ decrease mitosis. B) Mitotic Index. Mitosis was evaluated by counting the total number of mitotic figures in histological sections stained with H&E of 10 microscopic fields (40X objective). Values represent the mean ± SD of control after 18 days of IL-δ treatment. C) Western blot of PCNA and c-P27 in HT29 xenograft. Immunochemical detection of PCNA and P27 and actin levels using a specific antibody and anti-rabbit IgG antibody conjugated with peroxidase. (D) Quantification of PCNA and P27 levels by densitometry scanning of the immunoblots. Values were normalized with an anti-b-actin antibody. Results are expressed as means ± SD from three independent experiments. E) Caspase-3 activity. Caspase-3 activity was measured after 18 days of IL-δ treatment. Data are expressed as means ± SD from four independents experiments (* $p < 0.05$ versus control).

FIGURE 2

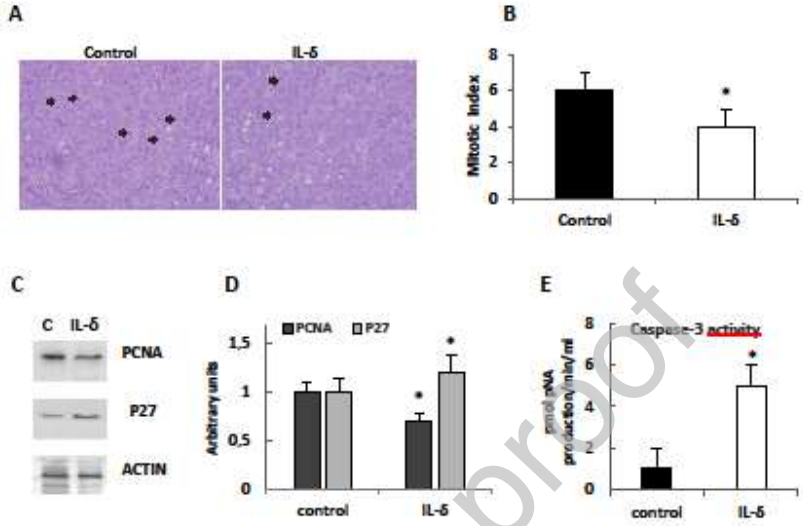

Figure 3: **IL-δ treatment decreases Microvessel Density (MVD).** Immunohistochemistry of CD31 marker. Mice were injected three days a week with vehicle or IL-δ during 18 and 30 days. Tumors were fixed in formol buffer after their extraction to carry over the desired morphological studies. A) Representative images of the immunohistochemistry of control and IL-δ after 18 and 30 days of treatment. B) Number of vessels per field after 18 and 30 days. MVD were measured by the average number of vessels per field counted in 10 random areas at 20X objective. C) Vascular Area (in pixel). Data are expressed as mean ± SD of four independent experiments (*p<=0.05 versus control).

FIGURE 3

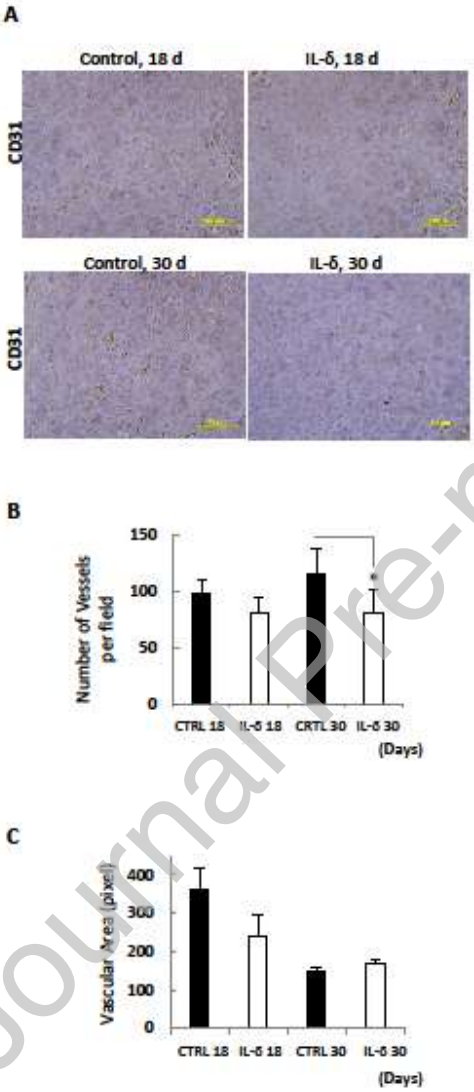

Figure 4: **IL-δ decreases VEGF and VEGF-R2 expression.** A) Real time PCR of VEGF-R2. B) Real time PCR of VEGF. Relative changes in gene expression were calculated according to the $2^{-\Delta\Delta Ct}$ method using GADPH as internal control. Data are presented as the means ± SD of 3 experiments (*p <0.05 as compared to respective control). C) Representative images of immunohistochemistry of VEGF. D) Immunohistochemistry analysis of VEGF. VEGF was quantified as the integrated intensity per field using the free software ImageJ. Five random fields per slide were selected at 40X objective. E) Representative images of immunohistochemistry of VEGF-R2. **F)** Immunohistochemistry analysis of VEGF-R2. VEGF-R2 was quantified as the integrated intensity per field using the free software ImageJ. Five random fields per slide were selected at 40X objective. Data are expressed as mean ± SD of four independent experiments (*p<0.05, **p<0.01 versus control group at each time of treatment).

FIGURE 4

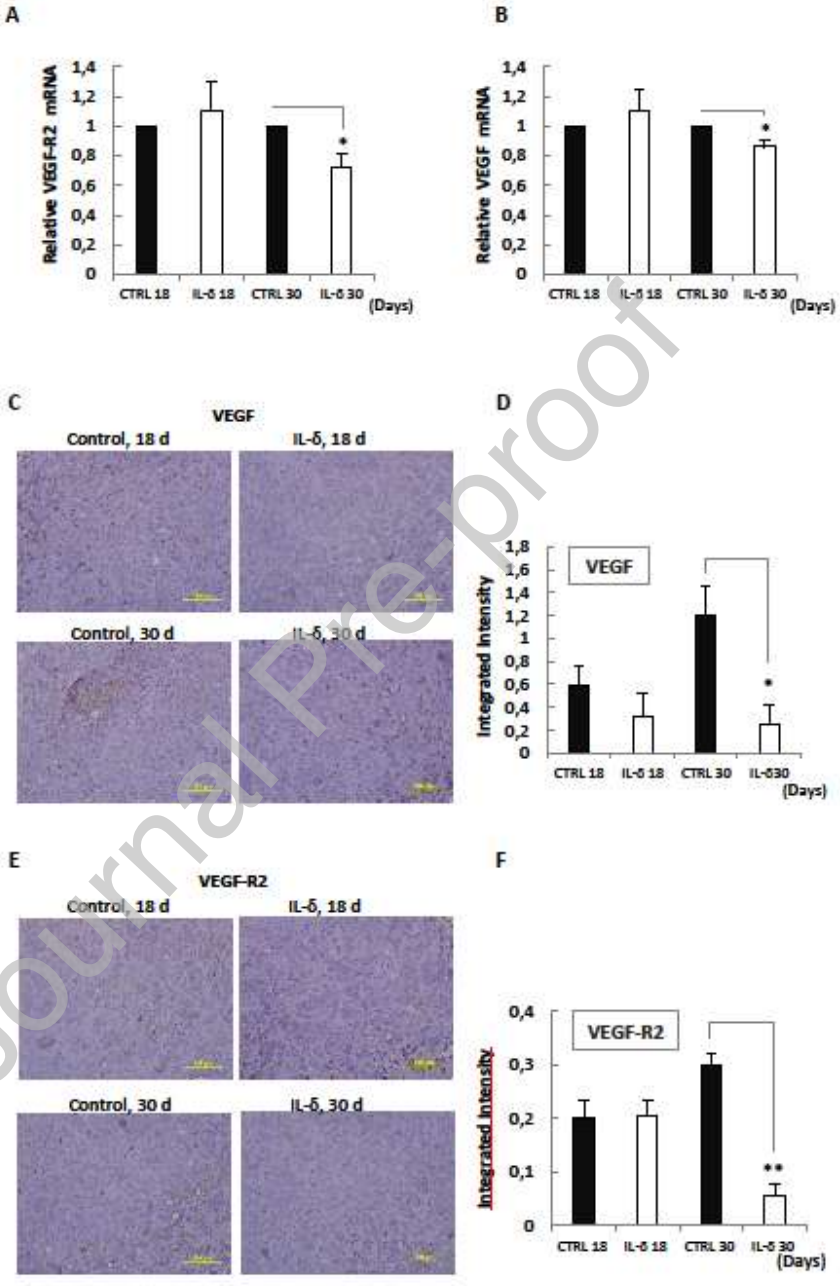

Figure 5: IL-δ increase VEGF-R1 and Ang-1 expression. VEGF-R1 and Ang-1 mRNA levels were determined by real time PCR. Relative changes in gene expression were calculated according to the $2^{-\Delta\Delta Ct}$ method using GADPH as internal control. Data are presented as the means ± SD of three experiments (* $p < 0.05$, and ** $p < 0.01$ versus control group at each time of treatment).

FIGURE 5